ACS OMEGA

http://pubs.acs.org/journal/acsodf

Article

Infrared and Terahertz Spectroscopic Investigation of Imidazolium, Pyridinium, and Tetraalkylammonium Tetrafluoroborate Ionic Liquids

Toshiki Yamada* and Maya Mizuno

Cite This: *ACS Omega* 2022, 7, 29804−29812

Read Online

ACCESS | Metrics & More | Article Recommendations | Supporting Information

ABSTRACT: We performed terahertz time-domain spectroscopy and infrared spectroscopy of imidazolium-based, pyridinium-based, and tetraalkylammonium-based tetrafluoroborate ionic liquids to study their characteristic intermolecular and intramolecular vibrational modes to clarify interactions between various cations and the tetrafluoroborate anion. It was found that the central frequency of the intermolecular vibrational band for these ionic liquids has a relatively high frequency, ranging from 90 to 100 cm^{-1}. In the 900−1150 cm^{-1} range, the intramolecular vibrational absorption band of the 3-fold degenerate mode of tetrafluoroborate anions in the ionic liquids was observed. Although the tetrafluoroborate anion is attributable to one of the weakly coordinated anions, the spectroscopic splitting behavior of the 3-fold degenerate mode differs depending on the cation species. It was revealed that the degenerate mode is very sensitive to local interactions between the tetrafluoroborate anion and each cation.

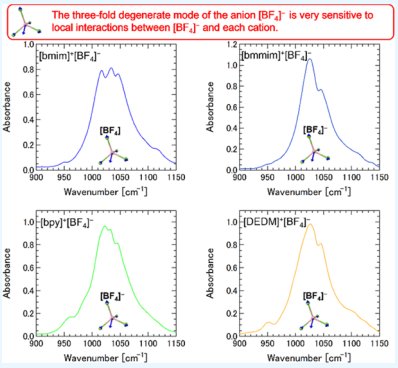

INTRODUCTION

Ionic liquids have unique characteristics such as a wide liquid temperature range, extremely low vapor pressure, high electrical conductivity, and excellent thermal stability. Ionic liquids also have excellent solvent properties in catalytic reactions and the dissolving of biopolymers, they are a lubricating liquid, and they are a nonvolatile refractive index matching medium.[1−6]

It is expected that the characteristics of ionic liquids will enable a wide range of scientific and industrial applications.[7−9] Understanding the noncovalent interactions of ionic liquids and the structures of ionic liquids is extremely important in understanding the unique properties of ionic liquids.[10,11] Therefore, various spectroscopic methods such as dielectric spectroscopy,[12,13] infrared (IR) and Raman spectroscopy,[14−28] NMR spectroscopy,[29,30] X-ray diffraction,[31,32] far-infrared (FIR) spectroscopy,[33−36] terahertz time-domain spectroscopy (THz-TDS),[37−40] and various kinds of nonlinear optical spectroscopy[41,42] have been applied to ionic liquids together with computer simulations.[43−52]

We have so far performed IR spectroscopy, FIR spectroscopy, and THz-TDS for a wide range of aprotic 1-methyl-3-alkylmethylimidazolium ionic liquids to systematically investigate their physical properties.[23−25,39,40] Intermolecular vibrations at low frequencies mainly originate from the interaction between cations and anions due to pure Coulomb interaction and local, directional hydrogen-bonding interactions. It was found that the central frequency ω of the intermolecular vibration based on the simple harmonic oscillator model ($\omega = (k/\mu)^{1/2}$) is determined based on the essential contribution of the reduced mass μ calculated from the masses of the methylimidazolium cation $[mim^+]$ and the anion $[A^-]$ as well as the force constant k. Thus, the central frequency ω of the intermolecular vibrational band was determined based on the properties of Coulomb liquids, although the strength of the cation−anion interaction is modified by local and directional hydrogen-bonding interactions. It has also been pointed out that electrostatic (Coulombic) interaction rather than hydrogen-bond-type interaction plays an important role in far-infrared spectral response due to inter-ionic vibrations.[36] On the other hand, the absorption frequencies of the $^+C(2)-H$ stretching vibrational mode of the methylimidazolium cation observed in the frequency range of 3000−3200 cm^{-1} and the out-of-plane bending vibrational mode of $^+C(2)-H$ the methylimidazolium cation observed in the frequency range of 700−950 cm^{-1} changes significantly depending on the strength of the anions' basicity or the strength of the hydrogen-bond-type interaction.[14,16−18,23,24] The tendencies of the absorption frequency changes in the $^+C(2)-H$ vibrational modes of the methylimidazolium cation due to hydrogen-bond-type interactions with anions showed a good correlation with the

Received: April 27, 2022
Accepted: August 10, 2022
Published: August 22, 2022

tendencies of the chemical shift of the $^{+}C(2)-H$ protons in ^{1}H-NMR and COSMO-RS (conductor-like screening model for realistic solvents) calculations.[21,50]

In this study, THz-TDS and IR spectroscopy were used to examine aprotic imidazolium tetrafluoroborate ionic liquid, aprotic pyridinium tetrafluoroborate ionic liquid, and aprotic tetraalkylammonium ionic liquid. We investigated the intermolecular vibrational absorption band and the characteristic intramolecular vibrational absorption band of these ionic liquids to clarify the interactions between various cations and the tetrafluoroborate anion. It is generally known that the 1-alkyl-3-methylimidazolium cation, the pyridinium cation, and the tetraalkylammonium cation have strong (Lewis) acidity in this order.[53] It is expected that 1-alkyl-2,3-dimethylimidazolium cation without $^{+}C(2)-H$ will be less acidic than the 1-alkyl-3-methylimidazolium cation. We discuss how the interactions between various cations and tetrafluoroborate anion appear in the IR and THz-TDS spectra. We found that the peak frequency in the intermolecular vibrational band for all of the ionic liquids studied was relatively high, ranging from 90 to 100 cm^{-1}, although it is generally known that the tetrafluoroborate anion is a weakly coordinating molecular anion.[16,18,54] It was found that the peak frequency of the intermolecular vibration band is essentially determined based on the characteristics as a Coulomb liquid, that is, based on the Coulomb cation−anion interaction with the minor role played by the local and directional hydrogen-bond-type interaction. We also studied the characteristic intramolecular vibration modes related to the intramolecular interaction of each ionic liquid. In particular, the peak splitting behavior of the three-hold degenerated vibrational mode of tetrafluoroborate anion observed at 900−1150 cm^{-1} differed depending on the cation species, although the tetrafluoroborate anion is weakly coordinated with each cation. Thus, the vibrational mode was found to be sensitive to local interactions between the tetrafluoroborate anion and each cation. As an extension of our previous work, we also studied ionic liquid systems in which a small amount of water was added to each ionic liquid.[23] It was revealed that the symmetric and antisymmetric stretching vibrations of water molecules observed at 3300−3800 cm^{-1} have the same frequency regardless of the cation species (interaction with each cation).

EXPERIMENTAL SECTION

IL samples such as 1-butyl-3-methylimidazolium tetrafluoroborate, 1-butyl-2,3-dimethylimidazolium tetrafluoroborate, 1-butylpyridinium tetrafluoroborate, 1-butyl-3-methylpyridinium tetrafluoroborate, 1-butyl-4-methylpyridinium tetrafluoroborate, and *N*,*N*-diethyl-*N*-methyl-*N*-(2-methoxyethyl)-ammonium tetrafluoroborate were used, as shown in Figure 1. The common abbreviations for anions and cations are also shown in Figure 1. The IL samples studied are aprotic imidazolium-, pyridinium-, and tetraalkylammonium tetrafluoroborate ionic liquids, which are in a liquid state at a room temperature of 25 °C. High-purity ionic liquid samples of 98% or higher were used.

To prepare the IL sample containing a small amount of water, 10 μL of water was added to the 500 μL ionic liquid sample and stirred for about 3 h before the experiment. The typical water concentration was 1.5 wt %. The concentration was the same, which was previously used in the investigation of the interactions between a small amount of water and ionic liquids.[23,55]

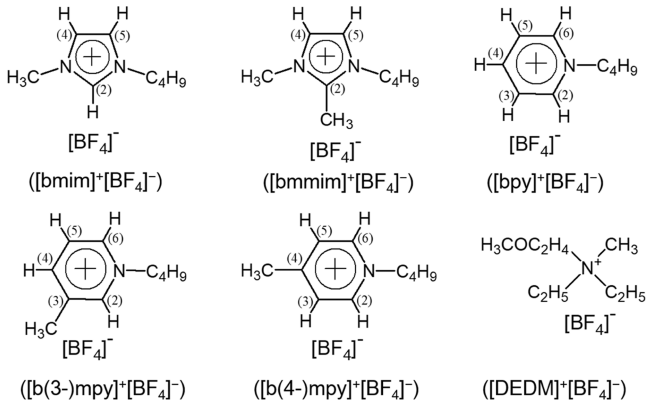

Figure 1. Ionic liquids used in this study.

An FTIR spectroscope (HORIBA, Ltd., FT-720) with an attenuated total reflection (ATR) unit (Smiths Detection, DuraScope) was used to measure the IR spectra of the IL samples. The THz-TDS apparatus (Advantest, TAS 7500SP) was used to measure the complex dielectric constant (Re ε, and Im ε) and absorption coefficient (α) spectra of the IL samples in the 14−120 cm^{-1} range. The absorption coefficient spectrum normalized by molar concentration (α/M) was obtained by measuring the density of the IL sample.[25,37,40]

In density functional theory (DFT) calculations, geometry was optimized at the B3LYP/6-311+G(d,p) level of theory with a charge of +1 (−1) for the cations (anions) of IL samples and a multiplicity of the singlet. Electrostatic potential, vibrational mode, and frequency were calculated at the same level of theory. The electrostatic potentials of $[bmim]^{+}$, $[bmmim]^{+}$, $[bpy]^{+}$, $[b(3\text{-})mpy]^{+}$, $[b(4\text{-})mpy]^{+}$, and $[DEDM]^{+}$ mapped onto their density surface (iso = 0.02) are calculated (see Figure S1). For $[bmim]^{+}$, $[bmmim]^{+}$, $[bpy]^{+}$, $[b(3\text{-})mpy]^{+}$, and $[b(4\text{-})mpy]^{+}$, the blue and light blue parts are localized in (hetero) aromatic rings, and the color of the butyl group part is lighter. In particular, the $^{+}C(2)-H$ part of $[bmim]^{+}$ is the deepest blue. The cation becomes electron-deficient mainly in the (hetero) aromatic ring part (blue and light blue parts) for $[bmim]^{+}$, $[bmmim]^{+}$, $[bpy]^{+}$, $[b(3\text{-})mpy]^{+}$, and $[b(4\text{-})mpy]^{+}$. Since Coulomb forces are the main driving structural feature of ILs, an interacting anion $[BF_4]^{-}$ may favorably reside at the (hetero) aromatic ring part (blue and light blue parts), especially in the deep (dark) blue part. For $[DEDM]^{+}$, there are many light blue parts as a whole, and the color of the methoxy group ($-O-CH_3$) part is lighter. For $[DEDM]^{+}$, an interacting anion $[BF_4]^{-}$ may favorably reside at the light blue part.

RESULTS AND DISCUSSION

Figure 2 shows the complex dielectric constant (Re ε and Im ε) spectra and absorption coefficient spectra (α) for $[bmim]^{+}[BF_4]^{-}$, $[bmmim]^{+}[BF_4]^{-}$, $[bpy]^{+}[BF_4]^{-}$, $[b(3\text{-})mpy]^{+}[BF_4]^{-}$, $[b(4\text{-})mpy]^{+}[BF_4]^{-}$, and $[DEDM]^{+}[BF_4]^{-}$ in the range of 14−120 cm^{-1}.

Changes in the curves are seen in the Re ε spectra of all IL samples below 40 cm^{-1} and between 80 and 120 cm^{-1}. The changes in the Re ε spectra correspond to the behavior below 40 cm^{-1} and the behavior between 80 and 120 cm^{-1} in the Im ε spectrum. Behavior below 40 cm^{-1} in the Im ε spectrum suggests the existence of a dielectric relaxation mode or a librational motion of a different cation.[13,57] On the other hand,

https://doi.org/10.1021/acsomega.2c02601
ACS Omega 2022, 7, 29804−29812

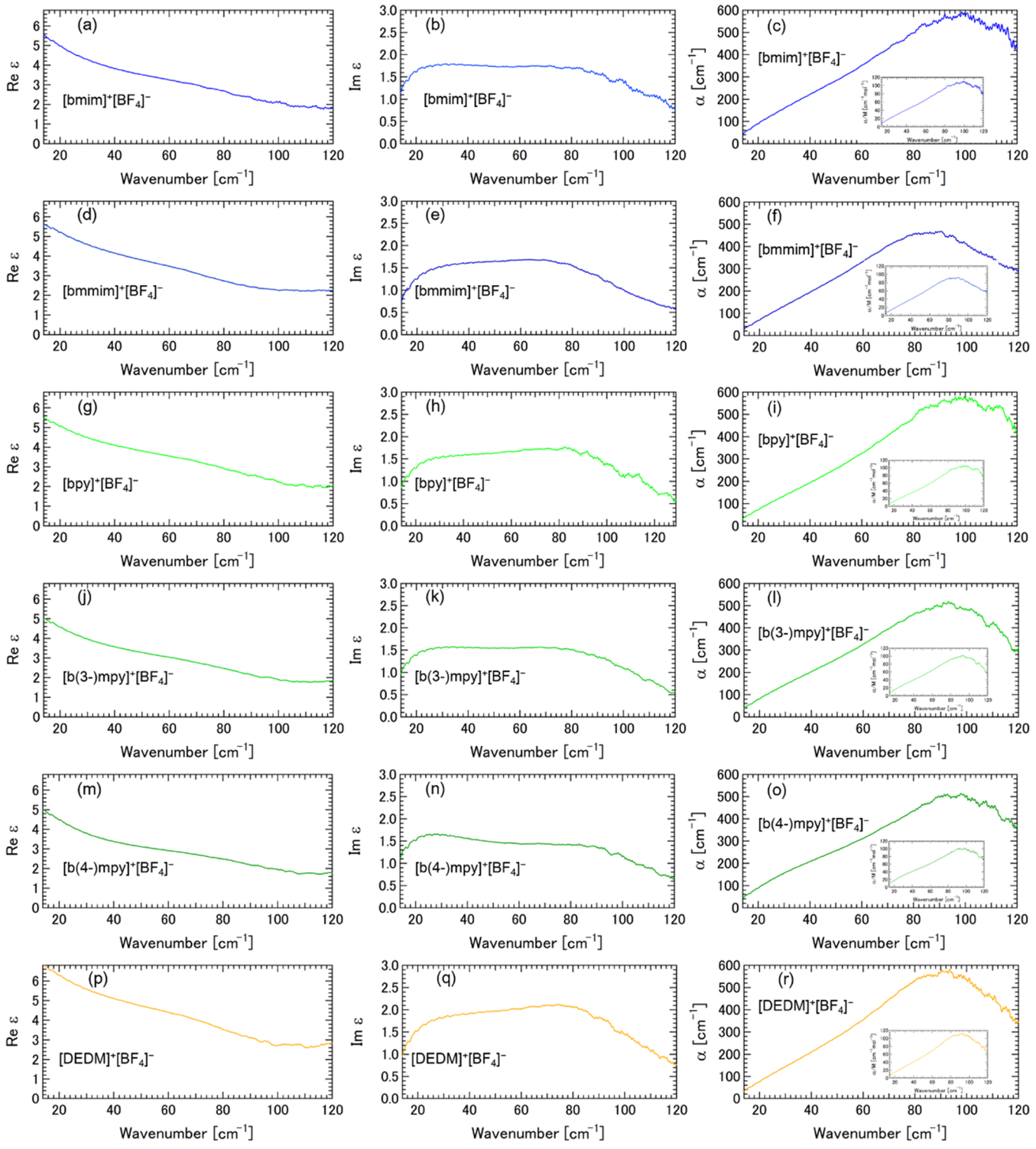

Figure 2. Complex dielectric constant (Re ε and Im ε) spectra and absorption coefficient spectra (α) for $[bmim]^+[BF_4]^-$ ((a–c)), $[bmmim]^+[BF_4]^-$ ((d–f)), $[bpy]^+[BF_4]^-$ ((g–i)), $[b(3\text{-})mpy]^+[BF_4]^-$ ((j–l)), $[b(4\text{-})mpy]^+[BF_4]^-$ ((m–o)), and $[DEDM]^+[BF_4]^-$ ((p–r)) in the range of 14–120 cm^{-1}.

the behavior of the changes between 80 and 120 cm^{-1} in the Im ε spectrum corresponds to the intermolecular vibrational mode between cations and anions, which corresponds to the main broad band of the absorption coefficient spectrum (α). According to our previous study, the same anion's imidazolium cation $[C_n mim]^+$ tends to exhibit larger magnitudes in Re ε below 40 cm^{-1}, where the number of n in C_n corresponds to the alkyl chain length.[40] For $[bmim]^+[BF_4]^-$, $[bmmim]^+[BF_4]^-$, $[bpy]^+[BF_4]^-$, $[b(3\text{-})mpy]^+[BF_4]^-$, and $[b(4\text{-})mpy]^+[BF_4]^-$, the (hetero) aromatic ring part of the cation is different, while the alkyl chain part, the butyl group (b) (n = 4 in C_n), is the same. In the present study, it was found that there was no significant difference in magnitudes of Re ε below 40 cm^{-1} for the five IL samples, which was consistent with our previous findings.[40] On the other hand, $[DEDM]^+$ is one of the tetraalkylammonium cations without a

https://doi.org/10.1021/acsomega.2c02601
ACS Omega 2022, 7, 29804−29812

Table 1. Effective Reduced Mass μ, $1/\mu^{1/2}$, Central Absorption Frequency [cm^{-1}], and Its Energy [meV] for IL Samples

	μ	$1/\mu^{1/2}$	wavenumber [cm^{-1}]	energy [meV]
$[mim]^+[BF_4]^-$	42.2	0.153	100	12.4
$[mmim]^+[BF_4]^-$	45.6	0.148	90	11.2
$[py]^+[BF_4]^-$	41.4	0.155	100	12.4
$[(3\text{-})mpy]^+[BF_4]^-$	44.9	0.149	94	11.7
$[(4\text{-})mpy]^+[BF_4]^-$	44.9	0.149	98	12.2
$[(C_2H_5)_2(CH_3)(C_2H_4)N]^+[BF_4]^-$	49.5	0.142	94	11.7

(hetero) aromatic ring moiety, and $[DEDM]^+$ is mainly composed of alkyl chain parts. The magnitudes in Re ε below 40 cm^{-1} for $[DEDM]^+[BF_4]^-$ have larger magnitudes than the other five IL samples, with a value of approximately 7 at 14 cm^{-1}. Thus, it was clarified that the magnitudes in Re ε below 40 cm^{-1} have larger magnitudes as the alkyl chain portions increase, even if the cation species are different. As far as the absorption coefficient (α) spectrum is concerned, IR spectroscopy, FIR spectroscopy, and THz-TDS were systematically performed on various 1-methyl 3-alkylmethylimidazolium ionic liquids with a different anion in our previous studies.[23,39,40] The main origins of the intermolecular vibration due to the interaction between the cation and the anion are the Coulomb interaction and the local and directional hydrogen-bonding interaction. We phenomenologically found that the central frequency ω of the intermolecular vibration based on the harmonic oscillator model ($\omega = (k/\mu)^{1/2}$) is determined by the essential contribution of reduced mass μ calculated from the masses of the methylimidazolium cation [mim^+] and the anion [A^-] as well as the intermolecular force constant k. For various 1-methyl 3-alkylmethylimidazolium ionic liquids with a different anion, the central frequency ω of intermolecular vibration depends little on the alkyl chain length of the 1-methyl 3-alkylmethylimidazolium cation, and therefore $[mim]^+$ as the effective mass of the cation is phenomenologically assumed. It is also supported that an interacting anion $[A]^-$ may favorably reside at the hetero aromatic ring part $[mim]^+$ from the electrostatic potential map.[56] Thus, the central frequency ω of the intermolecular vibration band is determined based on the characteristics of the Coulomb liquid, that is, phenomenologically based on the essential contribution of the reduced mass μ as well as the force constant k, although the local and directional hydrogen-bonding interaction may modify the strength of the cation−anion interaction.[33] It has been shown that this is systematically valid for various 1-methyl 3-alkylmethylimidazolium ionic liquids with a different anion.[23,39,40] As can be seen from the absorption coefficient (α) spectrum in Figure 2, $[bmim]^+[BF_4]^-$, $[bmmim]^+[BF_4]^-$, $[bpy]^+[BF_4]^-$, $[b(3\text{-})mpy]^+[BF_4]^-$, and $[b(4\text{-})mpy]^+[BF_4]^-$ have peaks at 100, 90, 100, 94, 98, and 94 cm^{-1}, respectively. A broad absorption band due to intermolecular interactions between the cations and anions was observed at relatively high frequencies. In previous studies of imidazolium-based ionic liquids, $[BF_4]^-$ is known to be weakly coordinated as a local interaction.[18] It is also known that the tetrafluoroborate anion is weakly coordinated as a local interaction in the pyridinium-based ionic liquid, and it is pointed out that the van der Waals effect, which is weaker than the hydrogen-bonding type interaction, dominates the interaction between the cation and the anion.[58] Tsuzuki et al. performed MP2/6-311G** level ab initio calculation for $[BF_4]^-$ complexes with 1-ethyl-3-metylimidazolium cation $[emim]^+$, 1-ethyl-2,3-dimethylimidazolium cation $[emmim]^+$, ethylpyridinium cation $[epy]^+$, and *N*-ethyl-*N*,*N*,*N*-trimethylammonium $[(C_2H_5)(CH_3)_3N]^+$.[46] The total interaction energies of the ion pair were −85.2, −81.8, −82.4, and −85.2 kcal/mol, respectively, and were not very different. The hydrogen-bonding type interaction with $^+C_2$−H of $[emim]^+$ was not essential for the attraction in $[emim]^+[BF_4]^-$ complex because the total interaction energy of $[emmim]^+[BF_4]^-$ complex was only 4% smaller than that of the $[emim]^+[BF_4]^-$ complex. We discuss the intermolecular vibration mode from the basic viewpoint of $\omega = (k/\mu)^{1/2}$. To proceed with the analysis, we consider the effective mass of the cation (m^+_{cation}) for $[bmim]^+$, $[bmmim]^+$, $[bpy]^+$, $[b(3\text{-})mpy]^+$, $[b(4\text{-})mpy]^+$, and $[DEDM]^+$. As in our previous study,[39,40] we assume the effective mass of $[mim]^+ = 82$ without the butyl group for $[bmim]^+$ phenomenologically because the center frequency of the intermolecular oscillation mode of $[C_nmim]^+[BF_4]$ ILs depends little on the alkyl chain length of the imidazolium cation, and it is also supported by the electrostatic potential map of $[bmim]^+$ (see Figure S1). The electrostatic potential maps for $[bmmim]^+$, $[bpy]^+$, $[b(3\text{-})mpy]^+$, and $[DEDM]^+$ were also used for reference (see Figure S1). For $[bmim]^+$, $[bmmim]^+$, $[bpy]^+$, $[b(3\text{-})mpy]^+$, and $[b(4\text{-})mpy]^+$, the cation becomes electron-deficient mainly in the (hetero)aromatic ring portion (blue and light blue parts) at which an interacting anion $[BF_4]^-$ may favorably reside. Thus, we assume the effective masses of $[mmim]^+ = 96$, $[py]^+ = 79$, $[(3\text{-})mpy]^+ = 93$, and $[(4\text{-})mpy]^+ = 93$ without the butyl group, for the cations of $[bmmim]^+$, $[bpy]^+$, $[b(3\text{-})mpy]^+$, and $[b(4\text{-})mpy]^+$, respectively. Thus, the effective mass corresponds to the mass of the (hetero)aromatic ring portion without the alkyl chain part. For $[DEDM]^+$, which is one of the tetraalkylammonium cations, we assume the effective mass of $[(C_2H_5)_2(CH_3)(C_2H_4)N]^+ = 115$, excluding the methoxy ($-OCH_3$) part with reference to the electrostatic potential map. The effective mass (m^-_{anion}) of the anion is assumed to be $[BF_4]^- = 86.8$, as previously. Although the concept of effective mass for the cations is phenomenological and somewhat ambiguous, we proceed with the analysis as described below.

Table 1 shows the effective reduced mass μ, $1/\mu^{1/2}$, the central absorption frequency [cm^{-1}], and the energy [meV] for the IL samples studied in this paper. It was found that there is no significant dispersion in the data in Table 1 when considering both the data obtained from the present study (the data in Table 1) and the data obtained from our previous studies[39,40] on various 1-metyl-3-alkyl-imidazolium ILs in the plot of the central absorption frequency versus $(1/\mu)^{1/2}$ (see Figure S2). Aprotic ILs having $[BF_4]^-$ and the different cations ($[bmim]^+[BF_4]^-$, $[bmmim]^+[BF_4]^-$, $[bpy]^+[BF_4]^-$, $[b(3\text{-})mpy]^+[BF_4]^-$, $[b(4\text{-})mpy]^+[BF_4]^-$, or $[DEDM]^+[BF_4]^-$) have a small local hydrogen-bonding type interaction, and the total interaction energy of the ion pair is not so large.[46,57] On the other hand, the central absorption frequencies of the

https://doi.org/10.1021/acsomega.2c02601
ACS Omega 2022, 7, 29804−29812

intermolecular vibration mode for $[bmim]^+[BF_4]^-$, $[bmmim]^+[BF_4]^-$, $[bpy]^+[BF_4]^-$, $[b(3\text{-})mpy]^+[BF_4]^-$, $[b(4\text{-})mpy]^+[BF_4]^-$, and $[DEDM]^+[BF_4]^-$ are in the 90−100 cm^{-1} range, as summarized in Table 1, and there is no significant dispersion in the present data in Figure S2, suggesting the minor role played by the local hydrogen-bond interaction to the central absorption frequency of the intermolecular vibration.

We consider the molar concentration-normalized absorption coefficient (α/M) against the effective molecular weight of an ion pair ($m^+_{cation}m^-_{anion}$). Here, α/M is equivalent to the absorption coefficient normalized by the number of ion pairs. The effective molecular weight of an ion pair is important because it is related to the size of the charge distribution of the ion pair and the physical size of the ion pair such as the average distance of the ion pair. We have so far reported that α/M at the center frequency of the intermolecular vibration is inversely proportional to the effective molecular weight ($m^+_{cation}m^-_{anion}$) for 1-alkyl-3-methyl-imidazolium ILs with various anions. The results of adding the corresponding data for IL samples used in this study to the previous data are shown (see Figure S3). Although there are some variations, it was clarified that the effective molecular weight of ILs that have $[BF_4]^-$ and different cations are relatively small, while the α/M values are relatively large. Thus, the results obtained in this study are consistent with the fact that α/M is inversely proportional to the effective molecular weight of the ion pair ($m^+_{cation}m^-_{anion}$).

Next, we will discuss the IR spectrum. In several studies,[14,17,18,21−23] it has been reported that the absorption band due to the $^+C(2)-H$ stretching vibrational mode of 1-methyl-3-alkyl-imidazolium cation observed in the frequency range of 3000−3300 cm^{-1} shows significant changes depending on the strength of the anion's basicity or the strength of the hydrogen-bonding type interaction. Figure 3a,b shows the IR

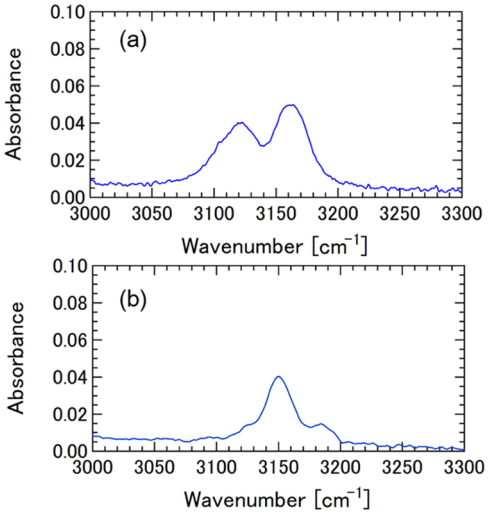

Figure 3. IR spectra in the range of 3000−3300 cm^{-1} for (a) $[bmim]^+[BF_4]^-$ and (b) $[bmmim]^+[BF_4]^-$.

spectra in the 3000−3300 cm^{-1} range for $[bmim]^+[BF_4]^-$ and $[bmmim]^+[BF_4]^-$, respectively. In this frequency range for $[bmim]^+[BF_4]^-$, $^+C(2)-H$ stretching vibrational mode, $^+C(4,5)-H$ antisymmetric stretching vibrational mode, and $^+C(4,5)-H$ symmetric stretching vibrational mode exist, and it is believed that the absorption by the stretching vibrational mode of $^+C(2)-H$ is on the lower frequency side. As can be seen in Figure 3b, the absorption on the lower vibration side disappears in $[bmmim]^+$, which does not have $^+C(2)-H$. $[BF_4]^-$ and $[Tf_2N]^-$ are relatively weakly coordinated anions, and it is known that the absorption of $[bmim]^+[BF_4]^-$ is very similar to that of $[bmim]^+[Tf_2N]^-$ in this frequency range. Comparing the IR spectrum of $[bmmim]^+[BF_4]^-$ in Figure 3b with $[bmmim]^+[Tf_2N]^-$ in the literature,[16] we recognize that they display very similar IR spectra.

Figure 4a,b shows the IR spectra of $[bmim]^+[BF_4]^-$ and $[bmmim]^+[BF_4]^-$ in the 700−900 cm^{-1} range, respectively.

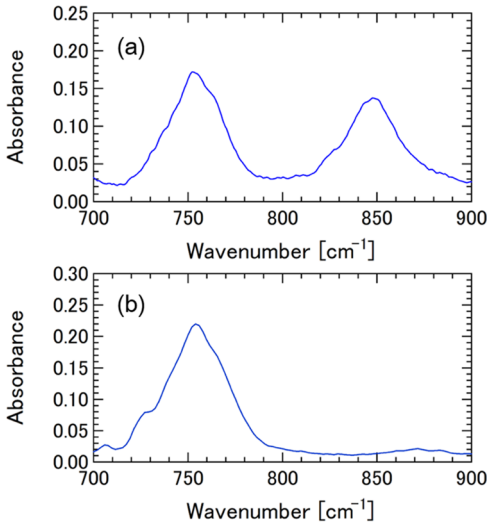

Figure 4. IR spectra in the frequency range of 700−900 cm^{-1} for (a) $[bmim]^+[BF_4]^-$ and (b) $[bmmim]^+[BF_4]^-$.

The absorption band with a peak around 850 cm^{-1} in Figure 4a is due to the out-of-plane bending vibrational mode of the $^+C(2)-H$ of the 1-methy-3-alkyl-limidazolium cation; the absorption band significantly changes depending on the strength of the anion's basicity or the strength of the hydrogen-bonding type interaction.[24] On the other hand, the absorption band with a peak around 750 cm^{-1} in Figure 4a is due to the out-of-plane bending vibrational mode of the $^+C(4,5)-H$ of the 1-methyl-3-alkyl-imidazolium cation. As can be seen in Figure 4b, the absorption band around 850 cm^{-1} disappears in $[bmmim]^+$, which does not have $^+C(2)-H$. On the other hand, the absorption band with a peak around 750 cm^{-1} in Figure 4b is due to the out-of-plane bending vibrational mode of $^+C(4,5)-H$ of $[bmmim]^+$. The out-of-plane bending vibrational mode of $^+C(4,5)-H$ was observed at almost the same frequency both for $[bmim]^+$ and $[bmmim]^+$. The above tendency was also well-reproduced in the calculation of the vibration modes of $[bmim]^+$ and $[bmmim]^+$ in the frequency range of 700−900 cm^{-1} (see Figure S4).

Figure 5a,b shows the IR spectra of $[bmim]^+[BF_4]^-$ and $[bmmim]^+[BF_4]^-$ in the frequency range of 1100−1200 cm^{-1}, respectively. The absorption band with a peak around 1170 cm^{-1} in Figure 5a is due to the in-plane bending vibrational mode of the $^+C(2)-H$ of the 1-methyl-3-alkyl-imidazolium cation. As we have previously shown, the in-plane bending vibrational mode of $^+C(2)-H$ is significantly insensitive to the strength of the anion's basicity or the strength of hydrogen-bonding type interaction, which are different from the $^+C(2)-H$ stretching vibrational mode and the $^+C(2)-H$ out-

https://doi.org/10.1021/acsomega.2c02601
ACS Omega 2022, 7, 29804−29812

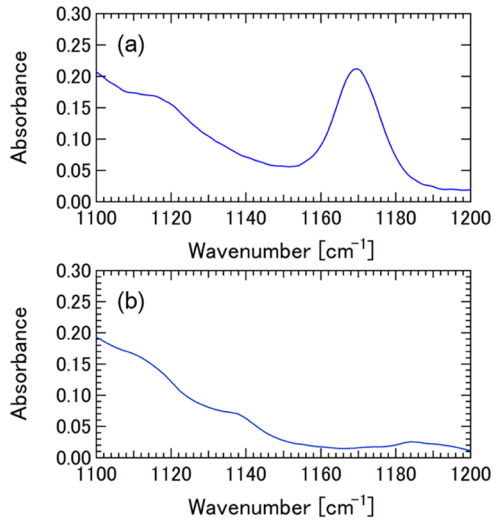

Figure 5. IR spectra in the frequency range of 1100−1200 cm^{-1} for (a) $[bmim]^+[BF_4]^-$ and (b) $[bmmim]^+[BF_4]^-$.

of-plane bending vibrational mode.[25] As can be seen in Figure 5b, we see that the absorption band around 1170 cm^{-1} disappears for $[bmmim]^+$, which does not have $^+C(2)-H$. In Figure 5a,b, the absorption tends to rise toward the low wavenumber side, which is due to the tail of the very strong absorption of the vibrational mode of $[BF_4]^-$ existing on the lower wavenumber side, which will be discussed later in detail.

Figure 6a−f shows the IR spectra in the range of 900−1150 cm^{-1} for $[bmim]^+[BF_4]^-$, $[bmmim]^+[BF_4]^-$, $[bpy]^+[BF_4]^-$, $[b(3\text{-})mpy]^+[BF_4]^-$, $[b(4\text{-})mpy]^+[BF_4]^-$, and $[DEDM]^+[BF_4]^-$, respectively. Absorption by the vibrational mode of the tetrafluoroborate anion $[BF_4]^-$ is observed in this range. The vibration mode of $[BF_4]^-$ is a 3-fold degenerate mode and has a very strong oscillator strength.[25,27] We previously showed that the absorption due to the vibrational mode is observed as three split peaks due to symmetry breaking due to the local interaction between $[BF_4]^-$ and 1-aklyl-3-methy-imidazolium cations.[25] Therefore, the vibration mode is expected to be very sensitive to local interactions. In $[bmim]^+[BF_4]^-$, as shown in Figure 6a, the degenerate vibrational mode of $[BF_4]^-$ was observed as three split peaks at 1017, 1033, and 1046 cm^{-1}. In $[bpy]^+[BF_4]^-$, as shown in Figure 6c, the degenerate vibrational mode was observed as three split peaks at 1022, 1032, and 1044 cm^{-1}, while the degree of splitting in $[bpy]^+[BF_4]^-$, as shown in Figure 6c, is smaller than in $[bmim]^+[BF_4]^-$, as shown in Figure 6a. The three spectra of $[b(3\text{-})mpy]^+[BF_4]^-$ in Figure 6d, $[b(4\text{-})mpy]^+[BF_4]^-$ in Figure 6e, and $[DEDM]^+[BF_4]^-$ in Figure 6f have a very similar spectral shape, with a peak at 1026 cm^{-1} and a shoulder structure at 1045 cm^{-1}. The spectra for $[bmmim]^+[BF_4]^-$ in Figure 6b have a peak at 1026 cm^{-1} and a shoulder structure at 1044 cm^{-1} and have the smallest absorption bandwidth compared with the other spectra. Thus, it is presumed that the order of magnitude of the local interaction between $[BF_4]^-$ and each cation is $[bmim]^+[BF_4]^-$ > $[bpy]^+[BF_4]^-$ > ($[b(3\text{-})mpy]^+[BF_4]^-$, $[b(4\text{-})mpy]^+[BF_4]^-$, and $[DEDM]^+[BF_4]^-$) > $[bmmim]^+[BF_4]^-$. The order is also consistent with the order of acidity of the cation.[53] We were able to observe the influence of local interactions by focusing on the 3-fold degenerate mode of $[BF_4]^-$, although, as shown by Tsuzuki et al.,[46,47] it is considered that there is no significant difference between $[BF_4]^-$ and each cation as the total

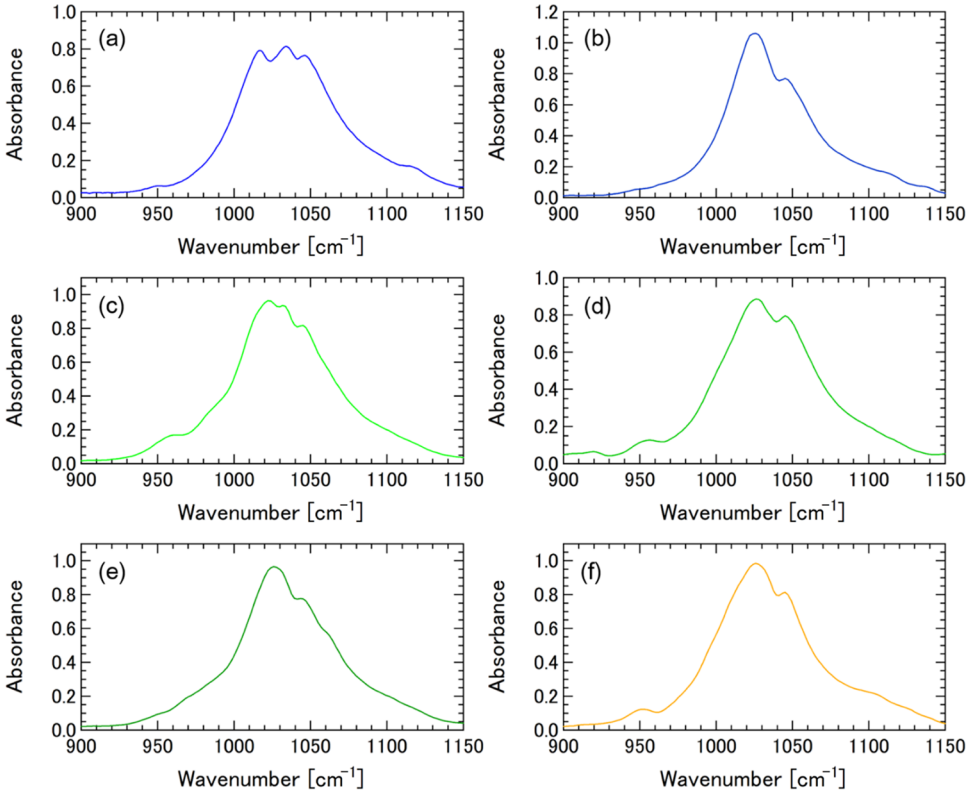

Figure 6. IR spectra in the range of 900−1150 cm^{-1} for (a) $[bmim]^+[BF_4]^-$, (b) $[bmmim]^+[BF_4]^-$, (c) $[bpy]^+[BF_4]^-$, (d) $[b(3\text{-})mpy]^+[BF_4]^-$, (e) $[b(4\text{-})mpy]^+[BF_4]^-$, and (f) $[DEDM]^+[BF_4]^-$.

https://doi.org/10.1021/acsomega.2c02601
ACS Omega 2022, 7, 29804−29812

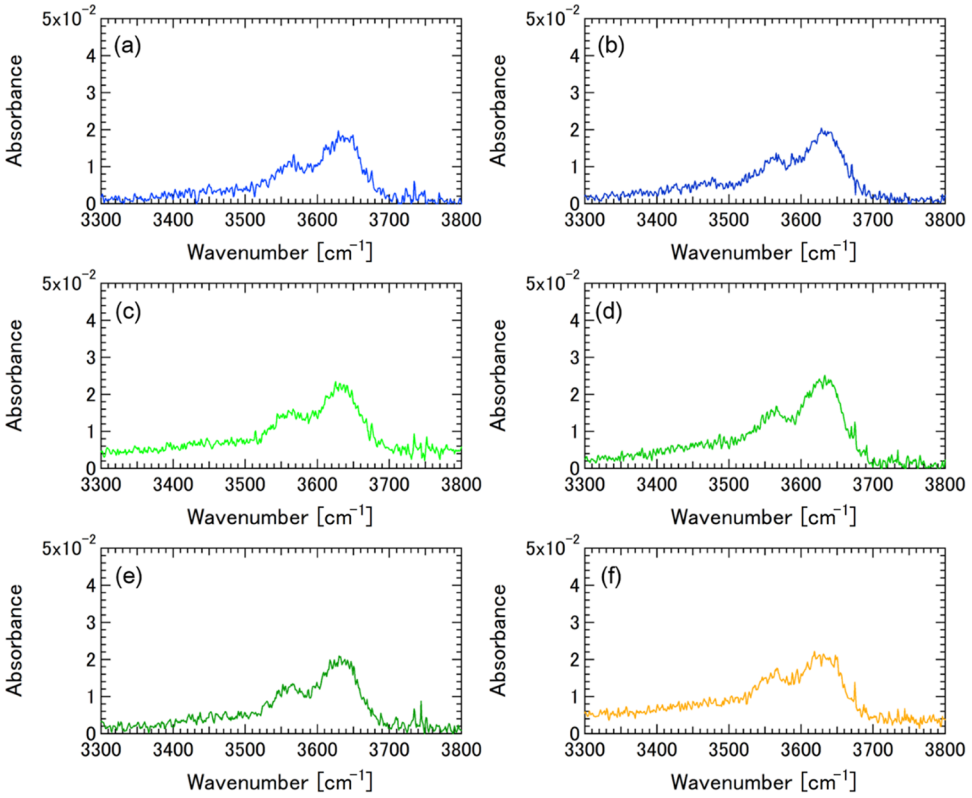

Figure 7. IR spectra in the range of 3300−3800 cm^{-1} of IL samples with a small amount of water for (a) [bmim]$^+$[BF$_4$]$^-$, (b) [bmmim]$^+$[BF$_4$]$^-$, (c) [bpy]$^+$[BF$_4$]$^-$, (d) [b(3-)mpy]$^+$[BF$_4$]$^-$, (e) [b(4-)mpy]$^+$[BF$_4$]$^-$, and (f) [DEDM]$^+$[BF$_4$]$^-$.

interaction energy, and the hydrogen-bonding type interaction with $^+$C(2)−H of [emim]$^+$ is not essential for the attraction in the [emim]$^+$[BF$_4$]$^-$ complex because the total interaction energy of the [emim]$^+$[BF$_4$]$^-$ complex is only 4% smaller than that of the [emmim]$^+$[BF$_4$]$^-$ complex.

Figure 7a−f shows the IR spectra of IL samples with a small amount of water in the range of 3300−3800 cm^{-1}. It is known that two absorption bands due to symmetric and antisymmetric stretching vibrational modes of water molecules are observed in the 3300−3800 cm^{-1} range.[55,59] In the ILs with a small amount of water added consisting of 1-alkyl-3-metyl-imidazolium cations and various anions, it has been shown that the frequencies of the absorption bands due to the water molecule's vibrational modes are red-shifted by the strength of the hydrogen-bonding interaction with the anions.[23] In the present study, we investigated the two absorption bands due to the symmetric and antisymmetric stretching vibrational modes of water molecules for the ILs with a small amount of water added consisting of [BF$_4$]$^-$ anion and various cations. As shown in Figure 7a−f, for all IL samples examined in this study, it was clarified that the two absorption bands due to the water molecules each have the same frequency, regardless of the local interaction with each cation or the acidity of each cation. An infrared predissociation study of the gas phase of the water-rich 1-metyl-3-butyl-imidazolium ILs was performed, and absorption bands reflecting the local interaction between the cation [bmin$^+$] and water molecules were observed for selected [bmin$^+$](H$_2$O)$_n$ (n = 1−8) clusters.[60] However, for bulk IL systems with a small amount of water, the absorption frequencies due to the symmetric and antisymmetric stretching vibrational mode of water molecules observed in the 3300−3800 cm^{-1} range are determined by local interactions with the anion rather than the cation.

CONCLUSIONS

The present study investigated intermolecular vibrational absorption bands and the characteristic intramolecular vibrational absorption bands of ILs such as [bmim]$^+$[BF$_4$]$^-$, [bmmim]$^+$[BF$_4$]$^-$, [bpy]$^+$[BF$_4$]$^-$, [b(3-)mpy]$^+$[BF$_4$]$^-$, [b(4-)mpy]$^+$[BF$_4$]$^-$, and [DEDM]$^+$[BF$_4$]$^-$ using THz-TDS and FTIR. We discussed how the interaction between the [BF$_4$]$^-$ anion and various cations ([bmim]$^+$, [bmmim]$^+$, [bpy]$^+$, [b(3-)mpy]$^+$, [b(4-)mpy]$^+$, and [DEDM]$^+$) appear in their respective spectra. The peak frequency of the intermolecular vibrational absorption band for the ILs was relatively high, ranging from 90 to 100 cm^{-1}, although [BF$_4$]$^-$ is one of the weakly coordinating anions. We found that the central frequency of the intermolecular vibration band is essentially determined based on the characteristics of a Coulomb liquid, that is, the Coulomb cation−anion interaction with the minor role played by specific hydrogen-bond-type interactions, regardless of cation species that have the different (Lewis) acidity. In the comparison of [bmim]$^+$[BF$_4$]$^-$ and [bmmim]$^+$[BF$_4$]$^-$, a $^+$C(2)−H stretching vibrational mode was observed in the 3000−3300 cm^{-1} range, a $^+$C(2)−H out-of-plane bending vibrational mode was observed in the 700−900 cm^{-1} range, and a $^+$C(2)−H in-plane bending vibrational mode was observed in the 1100−1200 cm^{-1} range and characteristic spectra were observed with and without each $^+$C(2)−H vibrational mode. In the range of 900−1150 cm^{-1}, an absorption band with very strong oscillator strength was observed due to the 3-fold degenerate vibrational mode of the [BF$_4$]$^-$ anion. The 3-fold degenerate vibrational mode was

https://doi.org/10.1021/acsomega.2c02601
ACS Omega 2022, 7, 29804−29812

observed as split peaks due to symmetry breaking due to the local interaction, although $[BF_4]^-$ is known as a weakly coordinated anion. It was revealed that the 3-fold degenerate vibrational mode is very sensitive to local interactions, and the degree of splitting varies depending on the interacting cation species. Judging from the spectral shape, the order of magnitude of the local interaction between $[BF_4]^-$ and each cation is $[bmim]^+[BF_4]^-$ > $[bpy]^+[BF_4]^-$ > ($[b(3\text{-})mpy]^+[BF_4]^-$, $[b(4\text{-})mpy]^+[BF_4]^-$, $[DEDM]^+[BF_4]^-$) > $[bmmim]^+[BF_4]^-$. Thus, the spectroscopic splitting behavior of the 3-fold degenerate mode of $[BF_4^-]$ could be a useful probe for understanding the local interactions in the ionic liquids with a weakly coordinated anion and provide insight into the nature of local interactions, which would promote experiments on dynamic aspects for the degenerate mode of $[BF_4^-]$ and computer simulations. In addition, research was also conducted on IL samples in which a small amount of water was added to each IL. It was revealed that the two bands, due to the symmetric and antisymmetric stretching vibrational modes of water molecules observed in the 3300−3800 cm^{-1} range, have the same frequencies, regardless of local interaction with each cation or the acidity of each cation. Thus, it was clarified that the two absorption bands of water molecules observed in the 3300−3800 cm^{-1} range are determined by local interactions with the anion rather than local interactions with the cation.

■ ASSOCIATED CONTENT

Supporting Information

The Supporting Information is available free of charge at https://pubs.acs.org/doi/10.1021/acsomega.2c02601.

Calculated electrostatic potentials of $[bmim]^+$, $[bmmim]^+$, $[bpy]^+$, $[b(3\text{-})mpy]^+$, $[b(4\text{-})mpy]^+$, and $[DEDM]^+$; plot of intermolecular vibration frequency versus $1/\mu^{1/2}$ obtained from the data both in the present and previous studies; molar concentration-normalized absorption coefficient (α/M) against effective molecular weight ($m^+_{cation}m^-_{anion}$) obtained from the data both in the present and previous studies; and calculated vibrational spectra for $[bmim]^+$ and $[bmmim]^+$ in the 700−900 cm^{-1} range (PDF)

■ AUTHOR INFORMATION

Corresponding Author

Toshiki Yamada − *Advanced ICT Research Institute, National Institute of Information and Communications Technology, Kobe 651-2492, Japan; Beyond 5G Research and Development Promotion Unit, National Institute of Information and Communications Technology, Koganei, Tokyo 184-8795, Japan;* orcid.org/0000-0002-9503-171X; Email: toshiki@nict.go.jp

Author

Maya Mizuno − *Radio Research Institute and Beyond 5G Research and Development Promotion Unit, National Institute of Information and Communications Technology, Koganei, Tokyo 184-8795, Japan*

Complete contact information is available at: https://pubs.acs.org/10.1021/acsomega.2c02601

Notes

The authors declare no competing financial interest.

■ REFERENCES

(1) Rogers, R. D.; Seddon, K. R. Ionic Liquids- Solvents of the Future? *Science* **2003**, *302*, 792−793.
(2) Castner, E. W., Jr.; Wishart, J. F. Spotlight on ionic liquids. *J. Chem. Phys.* **2010**, *132*, No. 120901.
(3) Fox, D. M.; Gilman, J. W.; Morgan, A. B.; Shields, J. R.; Maupin, P. H.; Lyon, R. E.; De Long, H. C.; Trulove, P. C. Flammability and Thermal Analysis Characterization of Imidazolium-Based Ionic Liquids. *Ind. Eng. Chem. Res.* **2008**, *47*, 6327−6332.
(4) Wang, H.; Gurau, G.; Rogers, R. D. Ionic liquid processing of cellulose. *Chem. Soc. Rev.* **2012**, *41*, 1519−1537.
(5) Zhou, Y.; Leonard, D. N.; Guo, W.; Qu, J. Understanding Tribofilm Formation Mechanisms in Ionic Liquid Lubrication. *Sci. Rep.* **2017**, *7*, No. 8426.
(6) Yamada, T.; Kaji, T.; Otomo, A. Orientation Imaging of Single Molecule at Various Ambient Conditions. *IEICE Trans. Electron.* **2013**, *E96-C*, 381−382.
(7) Jin, L.; Howlett, P. C.; Pringle, J. M.; Janikowski, J.; Armand, M.; MacFarlane, D. R.; Forsyth, M. An Organic Ionic Plastic Crystal Electrolyte for Rate Capability and Stability of Ambient Temperature Lithium Batteries. *Energy Environ. Sci.* **2014**, *7*, 3352−3361.
(8) Gorlov, M.; Kloo, L. Ionic Liquid Electrolytes for Dye-Sensitized Solar Cells. *Dalton Trans.* **2008**, *20*, 2655−2666.
(9) *Electrochemical Aspects of Ionic Liquids*; Ohno, H., Ed.; John Wiley & Sons:: Hoboken, NJ, 2011.
(10) Fumino, K.; Peppel, T.; Geppert-Rybczynska, M.; Zaitsau, D. H.; Lehmann, J. K.; Verevkin, S. P.; Köckerling, M.; Ludwig, R. The influence of hydrogen bonding on the physical properties of ionic liquids. *Phys. Chem. Chem. Phys.* **2011**, *13*, 14064−14075.
(11) Hayes, R.; Warr, G. G.; Atkin, R. Structure and nanostructure in ionic liquids. *Chem. Rev.* **2015**, *115*, 6357−6426.
(12) Wakai, C.; Oleinikova, A.; Ott, M.; Weingartner, H. How polar are ionic liquids? Determination of the static dielectric constant of an imidazolium-based ionic liquid by microwave dielectric spectroscopy. *J. Phys. Chem. B* **2005**, *109*, 17028−17030.
(13) Stoppa, A.; Hunger, J.; Buchner, R.; Hefter, G.; Thoman, A.; Helm, H. Interactions and dynamics in ionic liquids. *J. Phys. Chem. B* **2008**, *112*, 4854−4858.
(14) Jeon, Y.; Sung, J.; Seo, C.; Lim, H.; Cheong, H.; Kang, M.; Moon, B.; Ouchi, Y.; Kim, D. Structures of ionic liquids with different anions studied by infrared vibration spectroscopy. *J. Phys. Chem. B* **2008**, *112*, 4735−4740.
(15) Fumino, K.; Wulf, A.; Ludwig, R. Strong, Localized, and directional hydrogen bonds fluidize ionic liquids. *Angew. Chem., Int. Ed.* **2008**, *47*, 8731−8734.
(16) Lassègues, J. C.; Grondin, J.; Cavagnat, D.; Johansson, P. New interpretation of the CH stretching vibrations in imidazolium-based ionic liquids. *J. Phys. Chem. A* **2009**, *113*, 6419−6421.
(17) Wulf, A.; Fumino, K.; Ludwig, R. Comment on "New Interpretation of the CH stretching vibrations in imidazolium-based ionic liquids.". *J. Phys. Chem. A* **2010**, *114*, 685−686.
(18) Lassègues, J. C.; Grondin, J.; Cavagnat, D.; Johansson, P. Reply to the "Comment on 'New Interpretation of the CH stretching vibrations in imidazolium-based ionic liquids.'". *J. Phys. Chem. A* **2010**, *114*, 687−688.
(19) Gao, Y.; Zhang, L.; Wang, Y.; Li, H. Probing Electron Density of H-Bonding between Cation−Anion of Imidazolium-Based Ionic Liquid with Different Anions by Vibrational Spectroscopy. *J. Phys. Chem. B* **2010**, *114*, 2828−2833.
(20) Dong, K.; Song, Y.; Liu, X.; Cheng, W.; Yao, X.; Zhang, S. Understanding structures and hydrogen bonds of ionic liquids at the electronic level. *J. Phys. Chem. B* **2012**, *116*, 1007−1017.
(21) Cha, S.; Ao, M.; Sung, W.; Moon, B.; Ahlström, B.; Johansson, P.; Ouchi, Y.; Kim, D. Structures of Ionic Liquid-Water Mixtures Investigated by IR and NMR Spectroscopy. *Phys. Chem. Chem. Phys.* **2014**, *16*, 9591−9601.
(22) Paschoal, V. H.; Faria, L. F. O.; Ribeiro, M. C. C. Vibrational Spectroscopy of Ionic Liquids. *Chem. Rev.* **2017**, *117*, 7053−7112.

(23) Yamada, T.; Tominari, Y.; Tanaka, S.; Mizuno, M. Infrared Spectroscopy of Ionic Liquids Consisting of Imidazolium Cations with Different Alkyl Chain Lengths and Various Halogen or Molecular Anions with and without a Small Amount of Water. *J. Phys. Chem. B* **2017**, *121*, 3121−3129.
(24) Yamada, T.; Mizuno, M. Characteristic Spectroscopic Features due to Cation-Anion Interactions Observed in the 700 − 950 cm^{-1} Range of Infrared Spectroscopy for Various Imidazolium-based Ionic Liquids. *ACS Omega* **2018**, *3*, 8027−8035.
(25) Yamada, T.; Mizuno, M. Infrared Spectroscopy in the Middle Frequency Range for Various Imidazolium Ionic Liquids: Common Spectroscopic Characteristics of Vibrational Modes with In-Plane $^{+}$C(2)−H and $^{+}$C(4,5)−H Bending Motions and Peak Splitting Behavior Due to Local Symmetry Breaking of Vibrational Modes of the Tetrafluoroborate Anion. *ACS Omega* **2021**, *6*, 1709−1717.
(26) Berg, R. W.; Deetlefs, M.; Seddon, K. R.; Shim, I.; Thompson, J. M. Raman and ab initio Studies of simple and binary 1-alkyl-3-methylimidazolium ionic liquids. *J. Phys. Chem. B* **2005**, *109*, 19018−19025.
(27) Holomb, R.; Martinelli, A.; Albinsson, I.; Lassegues, J. C.; Johansson, P.; Jacobsson, P. Ionic liquid structure: the conformational isomerism in 1-butyl-3-methyl-imidazolium tetrafluoroborate ([bmim][BF4]). *J. Raman Spectrosc.* **2008**, *39*, 793−805.
(28) Grondin, J.; Lassegues, J.-C.; Cavagnat, D.; Buffeteau, T.; Johansson, P.; Holomb, R. Revisited vibrational assignments of imidazolium-based ionic liquids. *J. Raman Spectrosc.* **2011**, *42*, 733−743.
(29) Remsing, R. C.; Wildin, J. L.; Rapp, A. L.; Moyna, G. Hydrogen bonds in ionic liquids revisited: $^{35/37}$Cl NMR studies of deuterium isotope effect in 1-n-butyl-3-methylimidazolium chloride. *J. Phys. Chem. B* **2007**, *111*, 11619−11621.
(30) Nanda, R.; Damodaran, K. A review of NMR methods used in the study of the structure and dynamics of ionic liquids. *Magn. Reson. Chem.* **2018**, *56*, 62−72.
(31) Santos, C. S.; Murthy, N. S.; Baker, G. A.; Castner, E. W., Jr. Communication: X-ray scattering from ionic liquids with pyrrolidinium cations. *J. Chem. Phys.* **2011**, *134*, No. 121101.
(32) Annapureddy, H. V. R.; Kashyap, H. K.; De Biase, P. M.; Margulis, C. J. What is the origin of the prepeak in the X-ray scattering of imidazolium-based room-temperature ionic liquids? *J. Phys. Chem. B* **2010**, *114*, 16838−16846.
(33) Wulf, A.; Fumino, K.; Ludwig, R.; Taday, P. F. Combined THz and Raman spectroscopy studies of imidazolium-based ionic liquids covering the frequency range 2−300 cm^{-1}. *ChemPhysChem* **2010**, *11*, 349−353.
(34) Fumino, K.; Wulf, A.; Ludwig, R. The cation−anion interaction in ionic liquids probed by far-infrared spectroscopy. *Angew. Chem., Int. Ed.* **2008**, *47*, 3830−3834.
(35) Wulf, A.; Fumino, K.; Ludwig, R. Spectroscopic evidence for an enhanced anion−cation interaction from hydrogen bonding in pure imidazolium ionic liquid. *Angew. Chem., Int. Ed.* **2010**, *49*, 449−453.
(36) Buffeteau, T.; Grondin, J.; Danten, Y.; Lassegues, J.-C. Imidazolium-based ionic liquids: Quantitative aspects in the far-infrared region. *J. Phys. Chem. B* **2010**, *114*, 7587−7592.
(37) Yamamoto, K.; Tani, M.; Hangyo, M. Terahertz Time-Domain Spectroscopy of Imidazolium Ionic Liquids. *J. Phys. Chem. B* **2007**, *111*, 4854−4859.
(38) Mou, S.; Rubano, A.; Paparo, D. Complex Permittivity of Ionic Liquid Mixtures Investigated by Terahertz Time-Domain Spectroscopy. *J. Phys. Chem. B* **2017**, *121*, 7351−7358.
(39) Yamada, T.; Tominari, Y.; Tanaka, S.; Mizuno, M.; Fukunaga, K. Vibrational Modes at Terahertz and Infrared Frequencies of Ionic Liquids Consisting of an Imidazolium Cation and a Halogen Anion. *Materials* **2014**, *7*, 7409−7422.
(40) Yamada, T.; Tominari, Y.; Tanaka, S.; Mizuno, M. Terahertz and Infrared Spectroscopy of Room-Temperature Imidazolium-Based Ionic Liquids. *J. Phys. Chem. B* **2015**, *119*, 15696−15705.
(41) Turton, D. A.; Hunger, J.; Stoppa, A.; Hefter, G.; Thoman, A.; Walther, M.; Buchner, R.; Wynne, K. Dynamics of imidazolium ionic liquids from a combined dielectric relaxation and optical Kerr effect study: Evidence for mesoscopic aggregation. *J. Am. Chem. Soc.* **2009**, *131*, 11140−11146.
(42) Roth, C.; Chatzipapadopoulos, S.; Kerle, D.; Friedriszik, F.; Lütgens, M.; Lochbrunner, S.; Kuhn, O.; Ludwig, R. Hydrogen bonding in ionic liquids probed by linear and nonlinear vibrational spectroscopy. *New J. Phys.* **2012**, *14*, No. 105026.
(43) Turner, E. A.; Pye, C. C.; Singer, R. D. Use of ab initio calculations toward the rational design of room temperature ionic liquids. *J. Phys. Chem. A* **2003**, *107*, 2277−2288.
(44) Liu, Z.; Huang, S.; Wang, W. A Refined force field for molecular simulation of imidazolium-based ionic liquids. *J. Phys. Chem. B* **2004**, *108*, 12978−12989.
(45) Wang, Y.; Li, H.; Han, S. Structure and conformation properties of 1-alkyl-3-methylimidazolium halide ionic liquids: A density-functional theory study. *J. Chem. Phys.* **2005**, *123*, No. 174501.
(46) Tsuzuki, S.; Tokuda, H.; Hayamizu, K.; Watanabe, M. Magnitude and directionality of interaction in ion pairs of ionic liquids: Relationship with ionic conductivity. *J. Phys. Chem. B* **2005**, *109*, 16474−16481.
(47) Tsuzuki, S.; Tokuda, H.; Mikami, M. Theoretical analysis of the hydrogen bond of imidazolium C2-H with anions. *Phys. Chem. Chem. Phys.* **2007**, *9*, 4780−4784.
(48) Dong, K.; Zhang, S.; Wang, D.; Yao, X. Hydrogen Bonds in Imidazolium Ionic Liquids. *J. Phys. Chem. A* **2006**, *110*, 9775−9782.
(49) Izgorodina, E. I.; Golze, D.; Maganti, R.; Armel, V.; Taige, M.; Schubert, T. J. S.; MacFarlane, D. R. Importance of dispersion forces for prediction of thermodynamic and transport properties of some common ionic liquids. *Phys. Chem. Chem. Phys.* **2014**, *16*, 7209−7221.
(50) Cláudio, A. F. M.; Swift, L.; Hallett, J. P.; Welton, T.; Coutinho, J. A. P.; Freire, M. G. Extended Scale for the Hydrogen-Bond Basicity of Ionic Liquids. *Phys. Chem. Chem. Phys.* **2014**, *16*, 6593−6601.
(51) Hunt, P. A. Quantum chemical modeling of hydrogen bonding in ionic liquids. *Top. Curr. Chem.* **2017**, *375*, No. 59.
(52) Izgorodina, E. I.; Seeger, Z. L.; Scarborough, D. L. A.; Tan, S. Y. S. Quantum chemical methods for the prediction of energetic, physical, and spectroscopic properties of ionic liquids. *Chem. Rev.* **2017**, *117*, 6696−6754.
(53) Ueno, K.; Tokuda, H.; Watanabe, M. Ionicity in ionic liquids: correlation with ionic structure and physicochemical properties. *Phys. Chem. Chem. Phys.* **2010**, *12*, 1649−1658.
(54) Johnson, C. J.; Fournier, J. A.; Wolke, C. T.; Johnson, M. A. Ionic liquids from the bottom up: Local assembly motifs in [EMIM][BF4] through cryogenic ion spectroscopy. *J. Chem. Phys.* **2013**, *139*, No. 224305.
(55) Köddermann, T.; Wertz, C.; Heintz, A.; Ludwig, R. The Association of Water in Ionic Liquids: A Reliable Measure of Polarity. *Angew. Chem., Int. Ed.* **2006**, *45*, 3697−3702.
(56) Matthews, R. P.; Welton, T.; Hunt, P. A. Hydrogen bonding and π-π interactions in imidazolium-chloride ionic liquid clusters. *Phys. Chem. Chem. Phys.* **2015**, *17*, 14437−14453.
(57) Xiao, D.; Hines, L. G., Jr.; Li, S.; Bartsch, R. A.; Quitevis, E. L.; Russina, O.; Triolo, A. Effect of cation symmetry and alkyl chain length on the structure and intermolecular dynamics of 1,3-dialkylimidazolium Bis(trifluoromethanesulfonyl)amide ionic liquids. *J. Phys. Chem. B* **2009**, *113*, 6426−6433.
(58) Joseph, A.; Thomas, V. I.; Zyla, G.; Padmanabhan, A. S.; Mathew, S. Theoretical probing of weak anion-cation interactions in certain pyridinium-based ionic liquid ion pairs and the application of molecular electrostatic potential in their ionic crystal density determination: A comparative study using density functional approach. *J. Phys. Chem. A* **2018**, *122*, 328−340.
(59) Cammarata, L.; Kazarian, S. G.; Salter, P. A.; Welton, T. Molecular states of water in room temperature ionic liquids. *Phys. Chem. Chem. Phys.* **2001**, *3*, 5192−5200.
(60) Voss, J. M.; Marsh, B. M.; Zhou, J.; Garand, E. Interaction between ionic liquid cation and water: infrared predissociation study of $[bmin]^{+}\cdot(H_2O)_n$ clusters. *Phys. Chem. Chem. Phys.* **2016**, *18*, 18905−18913.

https://doi.org/10.1021/acsomega.2c02601
ACS Omega 2022, 7, 29804−29812